Virchows Archiv (1995) 426:179–188

ORIGINAL ARTICLE

Jan Hinrich Braesen · Ulrike Beisiegel · Axel Niendorf

Probucol inhibits not only the progression of atherosclerotic disease, but causes a different composition of atherosclerotic lesions in WHHL-rabbits

Received: 9 May 1994 / Accepted: 21 October 1994

Abstract Watanabe heritable hyperlipidaemic (WHHL)-rabbits develop premature atherosclerosis due to an inborn defect of the low-density lipoprotein (LDL) receptor causing severe hypercholesterolaemia. Probucol, which possesses a lipid lowering and an antioxidative potency, has been shown to reduce the extent of atherosclerotic disease in this animal. The object of the present study was the detailed analysis of the cellular and non-cellular composition of atherosclerosic lesions in WHHL-rabbits treated with probucol when compared with untreated controls. In two independent sets of experiments, each consisting of one litter, a total number of 5 animals was fed a diet containing 1% (w/w) probucol. Four animals served as controls and 2 animals were sacrificed before treatment (at 2 and 4 months of age, respectively) to define the baseline level of the atherosclerotic disease. Morphometric analysis was employed in order to determine plaque area macroscopically by planimetry and plaque thickness and composition histologically, in 30 cross-sections of the aorta of each animal. In the group treated with probucol, a diminution of plaque area and thickness, as well as a decrease of foam cell and – especially in one experiment - necrotic content of atherosclerotic lesions, was observed. Plaques from aortas of animals treated with probucol consisted predominantly of smooth muscle cells and compact intercellular fibrous structures. Furthermore, as an additional characteristic feature of the "typical" probucol plaque, they usually lacked confluent necrotic cores. In comparison with untreated animals, there was also a decrease in intracellular apolipoprotein B (apo B) as determined by immunohistochemistry. These data confirm the antiatherosclerotic potency of probucol in the WHHL-rabbit. Moreover, it was demonstrated that there is a different type of atherosclerosis present in the group treated with probucol. The mechanism behind these shifts may be based on the antioxidative property as well as on direct effects of probucol on cellular plaque components.

Key words Atherosclerosis · Watanabe heritable hyperlipidaemic rabbit · Probucol · Antioxidants · Morphometric analysis

J.H. Braesen
Institute of Pathology, University Hospital Eppendorf, University of Hamburg, Martinistrasse 52, D-20246 Hamburg, Germany

U. Beisiegel
Department of Internal Medicine, University Hospital Eppendorf, University of Hamburg, Martinistrasse 52, D-20246 Hamburg, Germany

A. Niendorf (✉)
Institute of Pathology, University Hospital Eppendorf, University of Hamburg, Martinistrasse 52, D-20246 Hamburg, Germany

Introduction

The WHHL-rabbit is a well-established model for familial hypercholesterolaemia [51]. These animals develop early and accelerated atherosclerosis due to a mutation in the LDL-receptor gene [18] that is similar to the class II mutations in human familial hypercholesterolaemia [5]. This allows the study of the influence of endogenously elevated cholesterol levels on atherogenesis [6, 22]. In WHHL-rabbits, probucol has been shown to slow the progression of atherosclerosis as evaluated by aortic surface planimetry [7, 9, 23]. This effect appears to be independent of the cholesterol lowering property of this drug [7, 40]. Probucol shows a potent antioxidative effect in low density lipoproteins [32]. There is strong evidence that oxidation of lipoproteins triggers atherogenesis [46, 48]; endproducts of lipidperoxidation have been found within atherosclerotic plaques [1, 4, 21], circulating antibodies directed against oxidized LDL have been demonstrated [39], clinical studies show a positive correlation between susceptibility to LDL-oxidation and the development of premature atherosclerosis [35], antioxidants – including probucol – inhibit the progression of atherosclerotic disease [3, 7, 23, 29] and LDL from probucol-treated animals have a lower tendency to become oxidised [9, 13, 24, 34]. In WHHL-rabbits treated with probucol reduced plaque formation and decrease in LDL degradation in fatty streak lesions has been determined, suggesting the inhibition of foam cell

formation [31, 45]. To date there have been no reports of detailed histological analysis of the impact of probucol on the formation of atherosclerotic plaques in WHHL-rabbits.

The present study was undertaken to determine whether probucol affects only the extent of atherosclerotic disease or rather induces changes in the cellular and noncellular composition of atherosclerotic plaques. Complete aortas of WHHL-rabbits treated with probucol as well as control animals were analysed with respect to plaque area, thickness and composition using a morphometric technique.

Methods

A total of 11 homozygous WHHL-rabbits bred at the animal facilities of the Medical Hospital of the University of Hamburg was included in two experiments. Each experiment consisted of one litter. In the first experiment, one female WHHL-rabbit was sacrificed at the age of 4 months in order to define a baseline control. Two additional control animals (1 female, 1 male) received standard rabbit chow and further two (1 female, 1 male rabbit) were fed a chow containing 1% probucol (w/w) for a period of 6 months. Blood samples were taken five times during the experiment. At the age of 10 months all animals were sacrificed.

In the second experiment, 6 WHHL-rabbits were treated according to an analogous procedure: at the age of 2 months one female was sacrificed as baseline control, two rabbits (1 female, 1 male) received a standard rabbit chow, and 3 animals (1 female, 2 males) were fed the probucol-diet for 12 months. Blood samples were taken six times during this experiment. These 5 WHHL-rabbits were sacrificed at the age of 14 months. The experimental design for both experiments is demonstrated in Fig. 1A, B.

In addition, one 2-year-old female WHHL-rabbit was examined. The experimental procedure has been approved by an ethical comittee.

After overnight fasting, the animals were sacrificed by an i.v. injection (2–5 ml) of a barbiturate derivate (natrium-5-allyl-5-(1′ methyl-n-butyl)-2-thiobarbiturate). An incision in the ventral median line was made, the animals were exsanguinated by puncture of the vena cava. Blood was collected into vacutainers containing 1.5 mg dipotassium EDTA/ml blood. Total cholesterol was determined by a standard enzymatic assay (Boehringer, FRG, Merck, FRG). Aortas were dissected and fixed in 4% buffered formalin, cut open and the luminal surface was photographed for morphometrical analysis of the plaque area. Afterwards, each aorta was sliced into 30 cross-sections and 10 consecutive cross-sections were embedded in one paraffin block resulting in 3 paraffin blocks for each aorta.

The histochemical staining included haematoxylin eosin, Goldner's variant of Masson trichrome stain (Masson-Goldner), azan (Heidenhain), astra blue, elastica (Van Gieson's technique), silver method (Kossa), and Berlin-blue reaction according to standard methods. A special combined stain "Masson-Goldner trichrome-elastica-Kossa" was developed in order to allow the simultaneous detection of cellular components (smooth muscle cells, foam cells), intercellular matrix (elastic, collagenous connective tissue) and calcified necrosis. First, the calcified necrosis was visualized

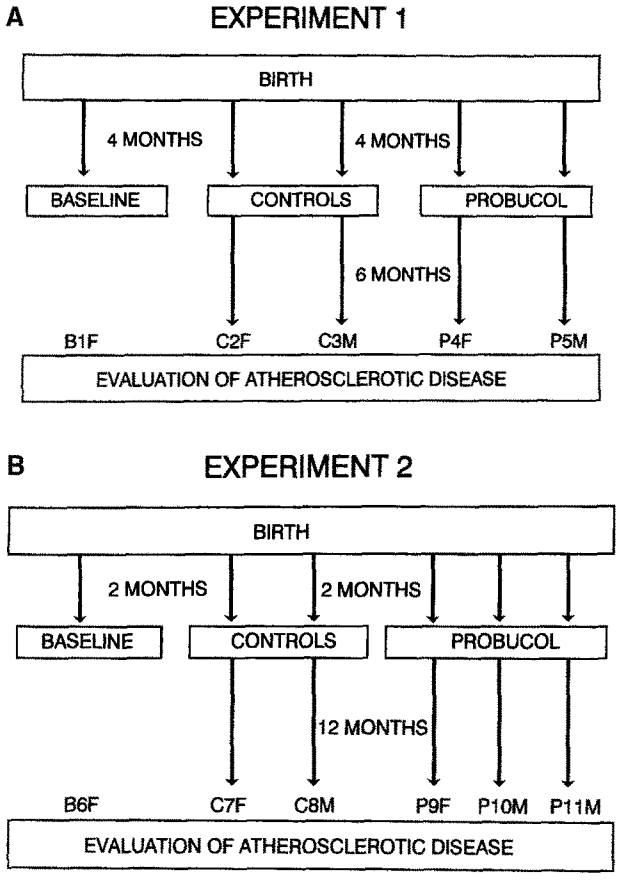

Fig. 1A, B Design of Experiment 1 and Experiment 2. (*B*, Baseline; *C*, Control; *P*, Probucol-treated; numbers of animals following one another; *F*, Female; *M*, Male). **A** Design of Experiment I. 5 homozygous WHHL-rabbits from one litter were fed a standard chow for 4 months, then one was sacrificed (B1F), two (1 female (C2F), 1 male (C3M)) received standard chow as controls, two (1 female (P4F), 1 male (P5M)) animals a 1% probucol containing diet for 6 months. At the age of 10 months these 4 animals were sacrificed and atherosclerotic disease was determined. **B** Design of Experiment II: 6 homozygous WHHL-rabbits were fed a standard chow for 2 months, then one female (B6F) was sacrificed, two animals (1 female (C7F), 1 male (C8M)) received standard chow as controls and three (1 female (P9F), 2 males (P10M, P11M), received a diet containing 1% probucol for 12 months. At the age of 14 months these 5 animals were sacrificed and atherosclerotic disease was determined

Fig. 2A, B Histological aspect demonstrating the resolution of the grid window used for morphometric analysis of plaque composition (**A**). (Combined Masson-Goldner trichrome-elastica-Kossa-stain, original magnification 250×). **B** Serial sections demonstrating comparability of the combined stain (middle) to immunohistochemical methods in validly differentiating smooth muscle cells (left, HHF 35) and macrophages (right, RAM 11). (original magnification 100×)

Fig. 7A, B Histological aspect of the "typical" plaque in probucol-treated animals (14 months old female). (*F*, Fibrous cap; *C*, Compact connective tissue core; *M*, Media; *IEL*, Internal elastic lamina). **A** Notice the fibrous cap (*F*) overlying a dense fibrous core (*C*), which lacks confluent necrosis and calcific material (Azan stain, original magnification 100×). **B** Detailed view of Fig. 7A. Notice the internal elastic lamina (IEL), which is bowed, but seems to be intact. Smooth muscle cells contain lipid vacuoles. Within the atheromatous core consisting of intercellular matrix (blue), there are some cholesterol clefts, but no necrotic core formation (Azan stain, original magnification 250×)

Fig. 8A, B Immunohistochemical stain of apoprotein B in a control and a probucol-treated WHHL-rabbit. **A** Plaque from 14 months old control female stained for apo B. Notice the unstained necrotic core (N) (*IEL*, Internal elastic lamina; *M*, Media; *L*, Luminal site) (original magnification 100×). **B** Plaque from probucol-treated animal stained for apo B (same lesion as Fig. 7). (*F*, Fibrous cap; *C*, Compact fibrous core; original magnification 100×)

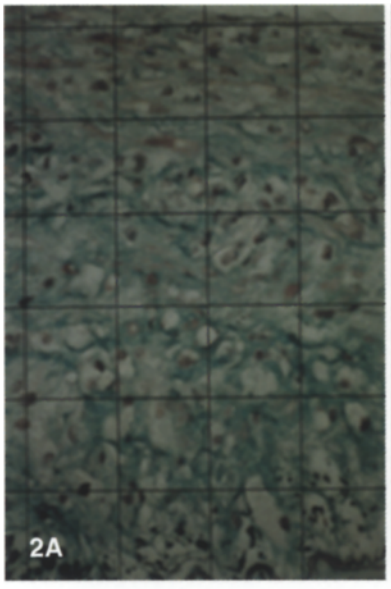
2A

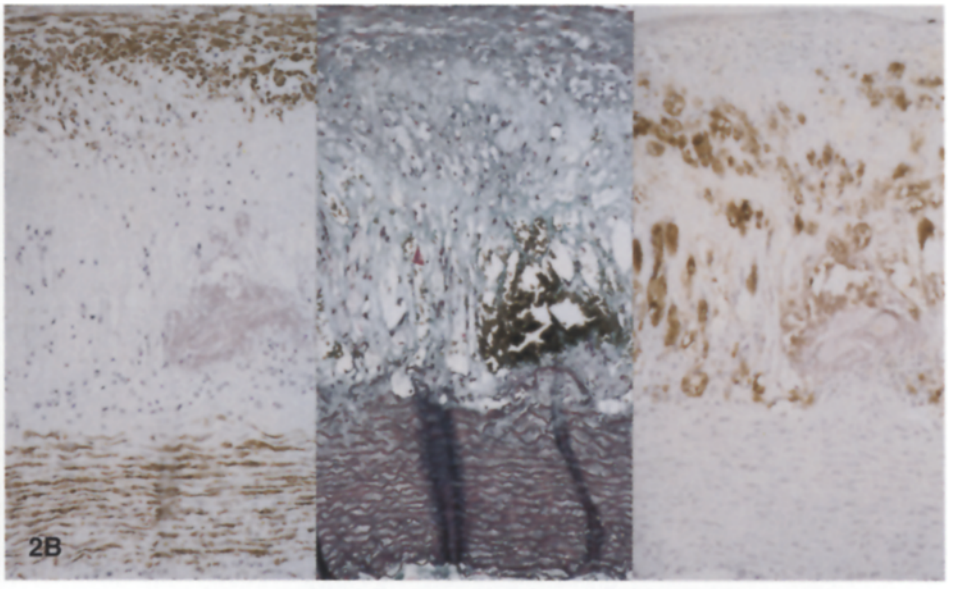
2B

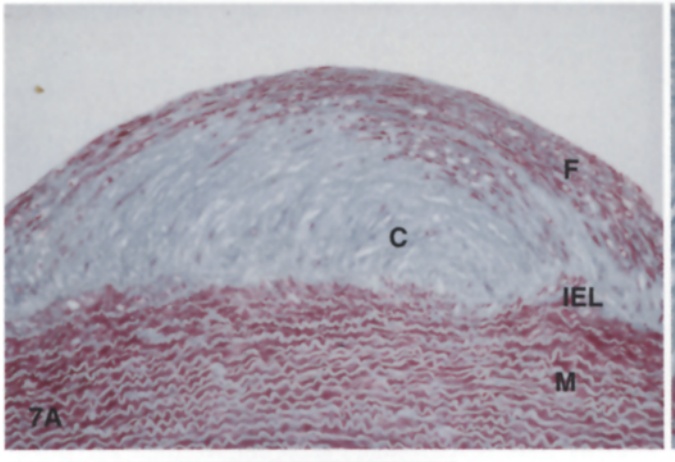
F
C
IEL
M
7A

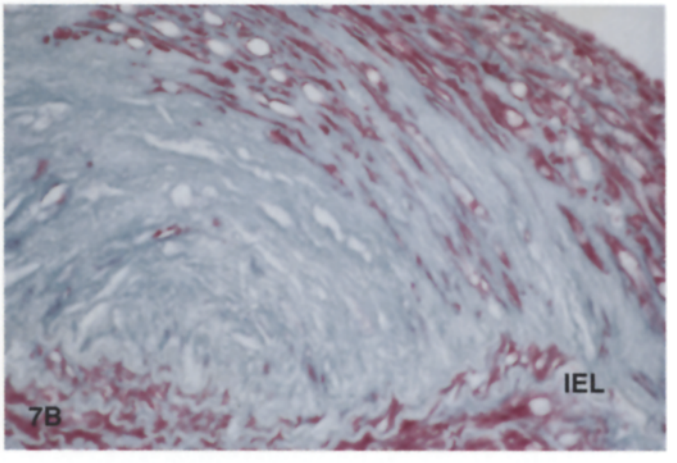
IEL
7B

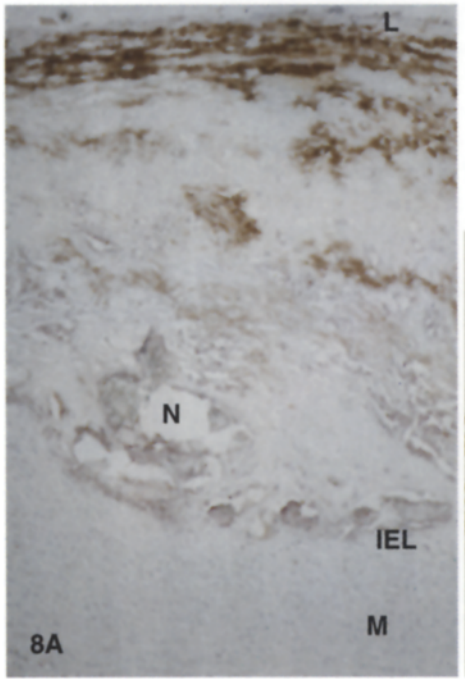
L
N
IEL
M
8A

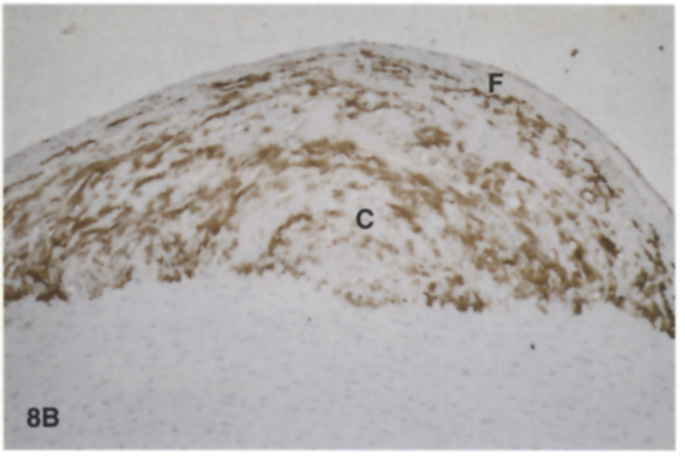
F
C
8B

by silver staining (Kossa); rehydrated sections (xylene for 5 min twice, 100% ethanol for 1 min twice, 96% ethanol for 1 min twice) were incubated in 5% silver nitrate for 30 min, subsequently rinsed in distilled water, for reduction, exposed to 1% hydrochinone and 5% sodium sulphite for 2 min and again rinsed in distilled water. Sections were fixed for 2 min in a solution of 5% aqueous sodium thiosulphate and rinsed with distilled water. Next, elastic fibres were stained according to van Gieson's technique in resorcin fuchsin (Weigert) for 10 min, rinsed for 1 min in running water and fixed in 80% ethanol. Masson-Goldner trichrome stain was started by an incubation in iron haematoxylin (Weigert) for 2 min, followed by rinsing with running water. Subsequently, sections were transferred to Ponceau's acid fuchsin azophloxin for 5 min, rinsed with 1% acetic acid and differentiated in Orange-G solution (2% phosphomolybdic acid and 2% Orange-G (Chroma, FRG) for 30 s, followed by a second rinse with 1% acetic acid. Intercellular matrix was then stained for 15 s in a 0.5% solution of light green (Merck, FRG) in 0.2% acetic acid. Finally sections were dehydrated in 96%, then 100% ethanol, at last xylene and mounted with Eukitt. This combination resulted in a black stain for calcified necrosis, green for connective tissue, violet for elastic fibres, red for muscle cells and a brown-red stain for nuclei.

Immunohistochemical staining of apo B (polyclonal goat anti-apo B, Immuno, FRG), HHF35 (monoclonal mouse anti-muscle actin, Enzo Diagnostics, New York, USA) and RAM11 (monoclonal mouse anti-rabbit macrophage, Dako Hamburg, FRG) was performed according to manufacturers recommendations (Vectastain Kit, Vector Laboratories, Burlingame, Calif., USA). Artefacts in staining apo B using normal rabbit serum (1:50) were excluded in preliminary tests by preblocking with PBS and 1 M sodium chloride, respectively.

Morphological variables were analysed using a computer based processing system (Kontron, Videoplan imaging system). The plaque area was quantified by planimetry of surface photographs and data expressed as percent area of total aortic surface. The plaque thickness of each cross-section was determined histologically at intervals of 1 mm; only values above 10 µm were used for statistic evaluation. Plaque composition was analysed by counting (grid counts=gc) the following components of the entire cross sectional plaque area at a 200-fold magnification using a grid-window (10×10 grids, grid size 0.06 mm): Smooth muscle cells (SMC), foam cells (FC), necrosis (NEC) and intercellular matrix (ICM) (combined stain). The resolution of the grid-window is demonstrated in Fig. 2A. Plaque components were identified according to the following criteria; SMC were identified as red-brown or violet to orange stained spindle-formed cells frequently containing lipid vacuoles. These cells lie within or upon the plaque, forming a fibrous cap. Characteristic for FC is a foamy looking cytoplasm caused by a large number of very small vacuoles. Macrophage-derived foam cells were differentiated from smooth muscle cells by the combined stain. The validity of this approach was demonstrated in a preliminary experiment, in which serial sections with the actin-specific antibody HHF35, the rabbit macrophage-specific antibody RAM11 and the combined stain were compared (Fig. 2B). NEC was recognized by black coloured calcified masses as identified by the Kossa stain or by the detection of cell debris. ICM was identified as green coloured fibrous or compact substance localized between cells or beneath the fibrous cap of the plaque. Apolipoprotein B deposition was determined using the same grid and magnification.

Data were stored and basic statistics (i.e. medians as well as first and third quartile) performed making use of the IPSS-statistic program of the University of Hamburg. Average cholesterol values were determined by planimetry of the area under the curve.

Results

Biochemical analysis

In both experiments the mean plasma cholesterol concentrations were lower in the probucol-treated animals (Table 1). The lower cholesterol levels were mostly due to an inhibition of increase of serum cholesterol levels (data not shown). Only one animal in experiment 1 (P4F) showed a marked decrease of total plasma cholesterol during probucol treatment (data not shown).

Table 1 Results of serum cholesterol and morphometric analysis of extent of atherosclerotic disease, each individual WHHL-rabbit of experiment 1, experiment 2 and of the additionally examined 2-year-old control female WHHL-rabbit. (*B*, Baseline; *C*, Control; *P*, Probucol; *F*, Female; *M*, Male) animals are numbered consecutively according to experiment 1, experiment 2 and the 2 year old WHHL-rabbit (C12F). Parameters include age (months), average serum cholesterol (*=mg/dl) deduced from area under the curve, plaque area (**=% of total aortic surface) and plaque thickness (***=µm, medians, first and third quartil in parentheses)

WHHL-No.	Months	Cholesterol*	Area**	Thickness***
B1F	4	665	50	125 (51–206)
C2F	10	822	53	138 (61–226)
C3M	10	933	48	235 (128–380)
P4F	10	611	22	93 (33–152)
P5M	10	772	30	91 (36–170)
B6F	2	449	0	16 (13–18)
C7F	14	683	49	168 (75–308)
C8M	14	682	40	220 (119–338)
P9F	14	580	27	53 (20–116)
P10M	14	505	18	99 (41–152)
P11M	14	578	12	71 (25–149)
C12F	24	742	93	346 (282–406)

Plaque area, plaque thickness and plaque composition in control animals

For data analysis, all values from baseline and control animals were first arranged according to their age in order to define stages of development of atherosclerosis and plaque composition at a certain age (Fig. 3A and B). At 2 months, there was no macroscopically visible plaque but a small increase in intimal thickness was determined by histological examination. Plaque thickness increased more than 20 fold within 22 months (from 2 to 24 months of age: 16 µm to 346 µm). Aortas of female rabbits showed a constant increase in plaque thickness, whereas plaque area did not differ between 4 and 14 months (4 months: 50%, 10 months: 53%, 14 months: 49%). Males of this age showed a greater plaque thickness, but less plaque area than the female rabbits (10 months: male 48%/235 µm, female 53%/138 µm; 14 months: male 40%/220 µm, female 49%/168 µm). However, in the two control males (10 and 14 months), no progression of atherosclerotic disease could be observed but rather a lower expression of atherosclerotic disease in the older animal (C8M) by means of plaque area and thickness. After 24 months the atherosclerotic lesions reached the greatest thickness (346 µm), occupying almost the entire aortic surface (93%).

The earliest lesion detectable by light microscopy in control animals were foam cells accumulating beneath the endothelium (Fig. 4A, 4 months). Next, isolated

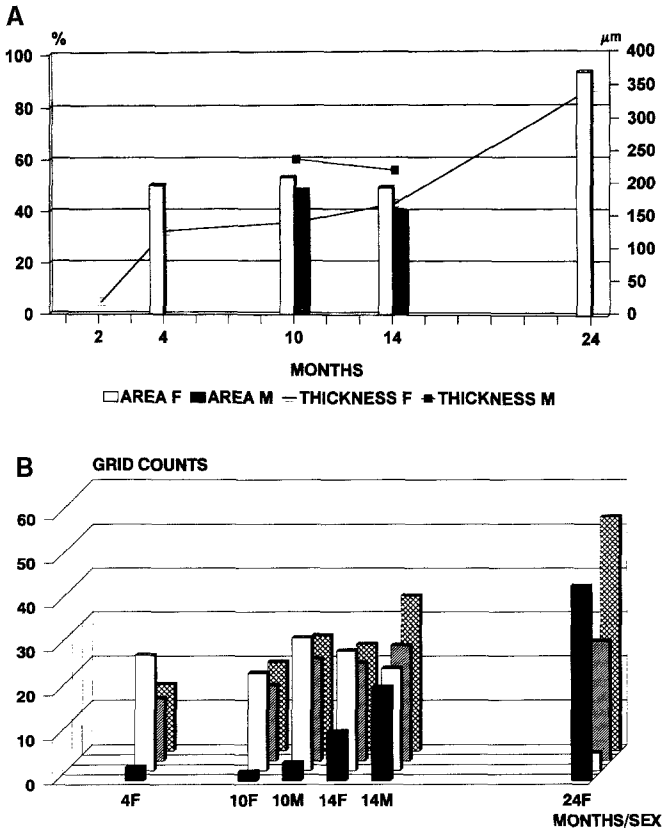

Fig. 3A, B Morphometric analysis of control animals depending on the age (bars representing medians). (*B*, Baseline; *C*, Control; *P*, Probucol; *F*, Female; *M*, Male). **A** Plaque area (% of total aortic surface) and plaque thickness (μm) of control rabbits, in dependence on the age. *White bars* represent plaque area in female rabbits, *black bars* in males. Box linking line shows plaque thickness in females, line between filled boxes plaque thickness in males. **B** Plaque composition (grid counts) of control animals, in dependence on the age: *black bars* show necrosis (NEC), *white bars* foam cells (FC), *hatched bars* show number of smooth muscle cells (SMC) and *squared gray bars* intercellular matrix (ICM)

smooth muscle cells appeared between foam cells (Fig. 4B, female, 4 months). In more developed plaques, massive smooth muscle cell accumulation was observed within the intimal space (Fig. 4C, female, 10 months). Simultaneously intercellular matrix appeared between smooth muscle cells. The smooth muscle cells showed intracellular lipids which were stored in much larger vacuoles when compared with foam cells (Fig. 4D, male, 10 months). Advanced plaques differed in appearance forming a fibrous cap and a core consisting of necrosis and surrounding foam cells (Fig. 4E, female, 14 months). Fig. 4F shows an atherosclerotic lesion stained with the combined "Masson-Goldner trichrome-Elastica-Kossa"-stain with a thrombohaemorrhagic complication (female, 14 months). In the aorta of the 2-year-old female rabbit, atherosclerotic lesions covered nearly the entire cross-section and impressed with a band-like zone consisting primarily of intercellular matrix and necrosis covered by a fibrous cap. Occasionally, there was a total lack of integrity in the media and foam cell accumulation occurred at the adventitial side of the vessel (Fig. 4G). Table 1 and 2 summarize the macroscopic appearance of surface lesions, medians and first and third quartile, respectively, of plaque thickness as well as of plaque composition for each individual animal.

Analysis of plaque composition in control animals is shown in Fig. 3B: In young animals, foam cells were the predominant constituent of plaques and necrosis was rare (4 months: 26 gc FC vs. 3 gc NEC, 10 months: 22 and 30 gc FC vs. 2 and 4 gc NEC). With advanced age of the animal, the number of smooth muscle cells as well as the amount of intercellular matrix increased moderately, with the increase of intercellular matrix prevailing over that of smooth muscle cells. The number of foam cells peaked at about one year. Almost simultaneously (at the age of 14 months) the necrosis content started to increase (10 months: 22/30 gc FC vs. 2/4 gc NEC; 14 months: 27/23 gc FC vs. 11/21 gc NEC; 24 months: 4 gc FC vs. 44 gc NEC).

Plaque area, plaque thickness and plaque composition in experiment 1

In experiment one, from 4 to 10 months, there was a progression of plaque thickness in control rabbits (125 μm to 138 and 235 μm, respectively), but plaque area remained almost constant (50% to 53 and 48%, respectively) (Fig. 5A; Table 1). Probucol treatment for 6 months beginning at the age of 4 months, when atherosclerotic lesions were already detectable, resulted in a diminution of plaque thickness and area below the baseline level (125 μm/50% vs. 93 μm/22% in female and 91 μm/30% in male). Analysis of plaque composition (Fig. 5B, Table 2) revealed a reduction in the number of foam cells in probucol-treated animals compared to controls (4 gc vs. 22 gc in female and 6 gc vs. 30 gc in male, respectively) and the baseline female (26 gc). Necrosis content was reduced compared to the controls (0 gc vs. 2 gc in female and 3 gc vs. 4 gc in male). Smooth muscle cells and intercellular matrix seemed unchanged when compared to controls. Intracellular apo B was not detectable by immunohistochemistry in probucol-treated animals. In contrast, extracellular deposition was not lower than baseline level and vaues did not differ between control and probucol-treated WHHL-rabbits (Table 2).

Plaque area, plaque thickness and plaque composition in experiment 2

In experiment two control rabbits showed an increase in plaque thickness (16 μm in female baseline animal vs. 168 μm in female and 220 μm in male control, respectively) (Fig. 6A, Table 1). Probucol treatment for a period of 12 months, beginning at the age of 2 months when only little intimal thickening was present (i.e. 16 μm, Table 1), resulted in an inhibition in the increase in plaque area and thickness (female: 53 μm/27% vs.

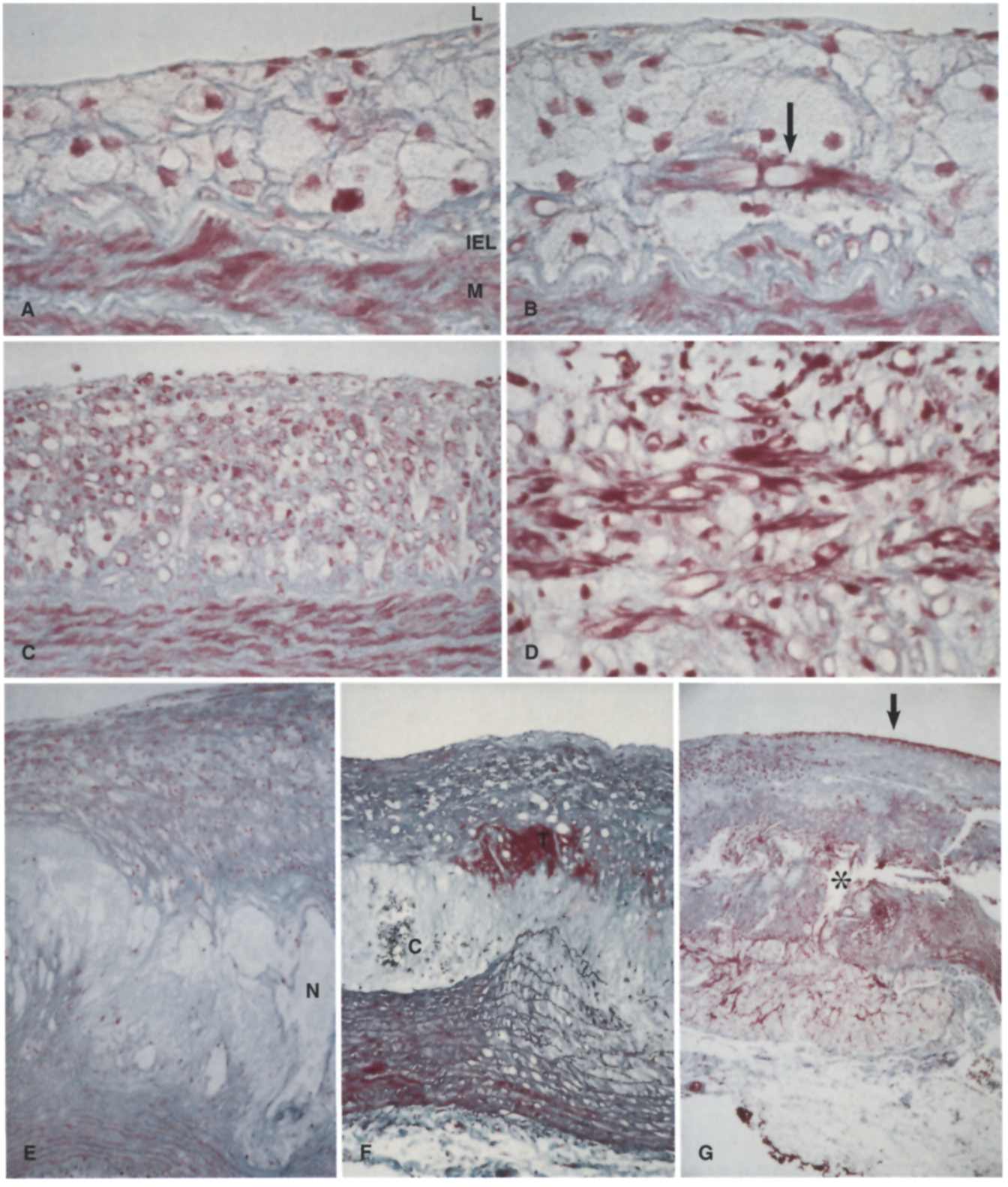

168 µm/49%; male: 99 µm/18% and 71 µm/12%, respectively vs. 220 µm/40%). Plaques from probucol-treated animals showed a lower expression of foam cells and
necrosis (females: 7 gc FC/2 gc NEC vs. 27 gc FC/11 gc NEC; males: 7 gc FC/3 gc NEC and 6 gc FC/6 gc NEC, respectively vs. 23 gc FC/21 gc NEC). Intercellular matrix was also reduced (females: 19 gc ICM vs. 24 gc ICM; males: 19 gc and 20 gc ICM, respectively vs. 35 gc ICM), whereas smooth muscle cell counts did not dif-

Table 2 Results of morphometric analysis of plaque composition – each individual WHHL-rabbit of experiment 1, experiment 2 and of the additionally examined 2-year-old control female WHHL-rabbit. (*B*, Baseline; *C*, Control; *P*, Probucol; *F* Female; *M* Male) animals are numbered consecutively according to experiment 1, experiment 2 and the 2 year old WHHL-rabbit (C12F). Parameters include smooth muscle cells (SMC), foam cells (FC), necrosis (NEC), intercellular matrix (ICM) and apolipoprotein B (APO B) (****=grid counts, all numbers are medians; first and third quartile in parentheses)

WHHL-No.	Months	SMC****	FC****	NEC****	ICM****	APO B****
B1F	4	14 (11–20)	26 (18–37)	3 (1–7)	15 (10–21)	7 (5–9)
C2F	10	17 (13–23)	22 (16–33)	2 (0–13)	20 (11–33)	9 (7–12)
C3M	10	23 (16–30)	30 (20–43)	4 (0–26)	26 (16–38)	14 (9–21)
P4F	10	22 (15–28)	4 (3–6)	0 (0–4)	24 (18–33)	12 (7–17)
P5M	10	18 (13–24)	6 (3–9)	3 (0–9)	23 (16–32)	11 (5–16)
B6F	2	0	0	0	0	0
C7F	14	22 (16–30)	27 (18–38)	11 (3–26)	24 (14–37)	13 (8–17)
C8M	14	26 (20–33)	23 (14–32)	21 (8–41)	35 (23–52)	11 (8–14)
P9F	14	18 (15–24)	7 (4–10)	2 (0–8)	19 (14–27)	10 (6–14)
P10M	14	19 (16–26)	7 (5–10)	3 (0–16)	19 (14–31)	11 (6–16)
P11M	14	23 (19–31)	6 (4–8)	6 (1–13)	20 (14–26)	9 (5–13)
C12F	24	27 (22–31)	4 (2–8)	44 (37–57)	53 (46–58)	12 (11–15)

fer significantly (Figs. 6B, 7A, B). In this experiment, intracellular apo B was also lowered below detectable levels, whereas extracellular apo B deposition was not altered quantitatively by probucol treatment (Table 2). In control animals, positive staining for apo B was detected predominantly within the fibrous cap and less in the underlying intercellular matrix (Fig. 8A). Necrotic cores usually lacked positive staining for apo B. Plaques from probucol-treated animals showed a more diffuse distribution and less staining within the fibrous cap (Fig. 8B).

Fig. 4 Development of atherosclerotic lesions in WHHL-rabbits. **A** Foam cell accumulation between endothelium and internal elastic lamina (IEL) in a 4 months old female WHHL-rabbit. (*L*, Luminal site; *M* Media) (Azan-stain, original magnification 630× oil.) **B** Foam cell accumulation within the intima and a single smooth muscle cell (*arrow*) lying between the foam cells, which contains lipid-vacuoles. (same animal as Fig. 4A, Azan-stain, original magnification 630× oil.) **C** Massive smooth muscle cell occurrence in the intima of a lesion shown with dispersed foam cells. Between smooth muscle cells intercellular matrix can be seen (blue). (10 months old female, Azan-stain, original magnification 250× oil.) **D** Photomicrograph demonstrating the contrast between macrophage-derived foam cells as inflated cells with foamy looking cytoplasm and smooth muscle cells containing much larger vacuoles. (10 months old male, Azan-stain, original magnification 400× oil). **E** Fibroatheroma from a 14 months of female WHHL-rabbit: a fibrous cap overlies a core containing foam cells, intercellular matrix and necrosis (*N*). (Azan-stain, original magnification 100×). **F** Complicated fibroatheroma stained with the combined stain. Beneath the fibrous cap formed by red spindle-shaped smooth muscle cells and dense green fibrous tissue, a thrombo-haemorrhagic complication (*T*) can be seen stained dense red. There is black stained calcified necrosis (*C*) within the less dense fibrous tissue, which contains atheromatous masses. Notice the fragmentation of elastic lamellae within the media, which contains few smooth muscle cells. (14 months old female, Masson-Goldner trichrome-elastica-Kossa-stain, original magnification 100×). **G** Complicated fibroatheroma from 2-year-old female WHHL-rabbit: a slim line of fibrin deposition can be detected upon the fibrous cap (*arrow*), which covers a zone containing foam cells, cholesterol-clefts and necrosis. The media has almost vanished and a rupture can be seen (*asterix*), rendering a continuity between foam cells within the plaque and a pool in the adventitia. (Azan-stain, original magnification 40×)

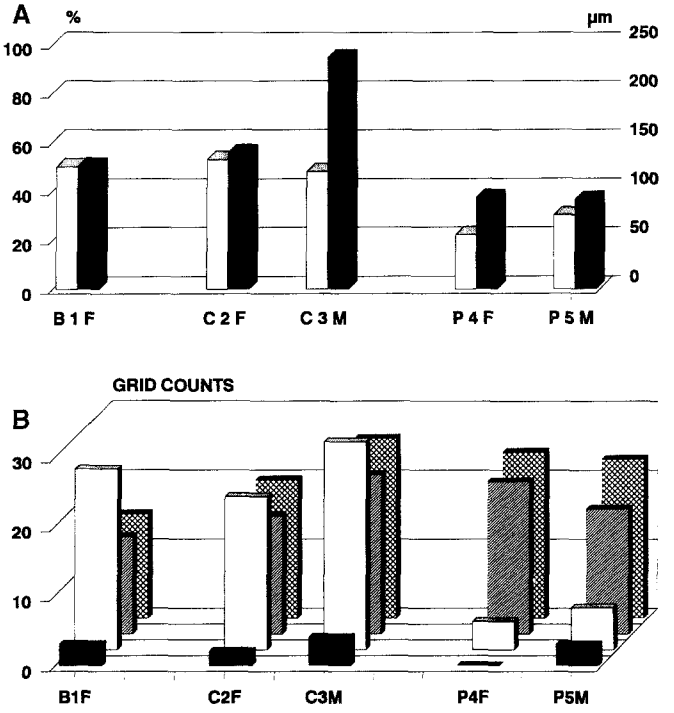

Fig. 5A, B Morphometric analysis of experiment 1 (animal numbers from left to right as in Fig. 1A). **A** Plaque area (white bars, % of total aortic surface) and plaque thickness (black bars, µm). **B** Plaque composition (grid counts) of experiment 1: *black bars* show necrosis (NEC), *white bars* foam cells (FC), *hatched bars* show number of smooth muscle cells (SMC) and *squared bars* intercellular matrix (ICM)

Discussion

The present study provides a detailed analysis of the composition of atherosclerotic lesions in WHHL-rabbits. In two independent experiments probucol caused an inhibition in the progression of atherosclerotic disease.

The development of atherosclerosis, as well as probucol-induced effects on atherogenesis, was investigated

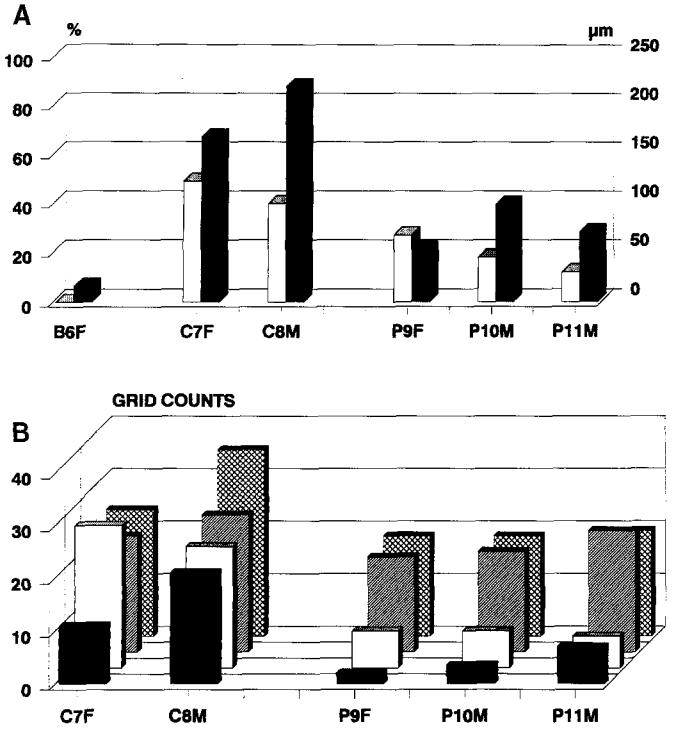

Fig. 6A, B Morphometric analysis of experiment 2 (animal numbers from left to right as in Fig. 1B). **A** Plaque area (*white bars*, % of total aortic surface) and plaque thickness (*black bars*, µm) of experiment 2. **B** Plaque composition of experiment 2 in grid counts: *black bars* show necrosis (NEC), *white bars* foam cells (FC), *hatched bars* show number of smooth muscle cells (SMC) and *squared bars* intercellular matrix (ICM)

with respect to plaque area, thickness and composition by means of morphometric analysis. In order to better determine the true extent of atherosclerotic disease, 30 cross-sections of the aorta of each animal were investigated. Our data show that the measurement of only one variable such as plaque area or plaque thickness may lead to an underestimation of the true dimension of this disease. As we observed that probucol reduced the extent of atherosclerosis in WHHL-rabbits, we investigated whether atherosclerotic plaques of probucol-treated animals are just smaller or whether they also differ with respect to their histological composition. The two cellular components that have been determined in our study have also been studied by other investigators [31, 50], who employed two monoclonal antibodies (i.e. RAM 11 and HHF 35) directed against antigens indicative for macrophages and smooth muscle cells. In a preliminary study we compared results from immunohistochemical staining using both antibodies to those obtained with our combined stain on serial sections (Fig. 2B). We found that the combined Masson-Goldner trichrome-elastica-Kossa-stain not only allows the differentiation between macrophage-derived foam cells and smooth muscle cells, but also (simultaneously) the identification of intercellular matrix and necrosis in one section. Thus, in this paper the term foam cell is exclusively used for cells of macrophage origin.

Using the approach described above, we analysed the control animals and one old (24 months) rabbit in order to confirm the validity of this method as a valuable tool for analysing the progression of atherosclerosis. A constant increase was shown in plaque thickness of female rabbits, whereas plaque area seemed not to change between 4 and 14 months. There were only two males as controls, which did not show comparable results. In the initial stages of this disease a predominance of foam cells was detected, followed by the additional appearance of nearly equal parts of smooth muscle cells and intercellular matrix. In more advanced lesions (24 months) the foam cell content was greatly decreased whereas the amount of necrosis increased. This shift at a certain age or point of plaque development is most likely due to the transition of macrophage-derived foam cells to necrosis. Studies investigating the origin of lipid vacuoles within the atheromatous core of atherosclerotic lesions provide evidence supporting this hypothesis [19]. Simultaneously, in the more advanced lesions, smooth muscle cells increased only slightly in number, whereas the amount of intercellular matrix increased more strongly. The fact that smooth muscle cells produce a constant amount of intercellular matrix [49], explains our observation of an disproportionate increase in intercellular matrix in comparison with the increase in the number of smooth muscle cells.

Probucol inhibited the progression of atherosclerotic disease. This can be deduced from both experiments in this study. Furthermore, results from experiment I, which included those animals who received probucol treatment in a more advanced stage of disease (4 months), suggest that this agent might even induce regression of pre-existing atherosclerotic lesions. Again, at a more advanced age (9 months), probucol treatment seems only to inhibit progression of atherosclerotic disease assessed by surface planimetry [9]. One can speculate that the amount of vital foam cells at the beginning of the regression-regimen plays a critical role in the potential regression of atherosclerotic plaques.

In both experiments probucol induced a shift in composition of cellular and extracellular constituents of plaques. The diminution of foam cells in plaques from probucol-treated WHHL-rabbits has been described previously [24, 31, 45], however without an precise quantification of this observation. In our study, the most striking finding is the quantitatively described reduction of foam cell number and necrosis that characterizes the structural difference of atherosclerotic plaques in probucol-treated animals. The typical plaque from probucol-treated WHHL-animals had a compact fibrous and relatively acellular core which usually lacked confluent necrotic areas and was covered by a dense fibromuscular cap (Fig. 7A, B).

These profound effects on the structural properties of atherosclerotic plaques in WHHL-animals may be based on direct effects of probucol on monocytes or macrophages [25, 46, 52], leading to an inhibition of the accumulation and subsequent destruction of macrophage-derived foam cells [46, 47], which results in necrosis. How-

ever, we might well be dealing with indirect probucol effects not mediated by cells, for example, reduction of serum cholesterol, which was observed here (Table 1). Although it has been shown that probucol reduces the extent of atherosclerotic disease independent of its cholesterol-lowering effect [7], the lipid-lowering effect might also contribute to a certain extent to the different atherosclerotic phenotype. However, on the basis of our morphological observations, it seems more likely that there are additional mechanisms of probucol action playing a role in generating different types of plaques in treated animals. Our analysis of the process of atherogenesis in control animals suggests, that smaller plaques should be rich in macrophage-derived foam cells, but the contrary was found in probucol-treated animals. What could be the mechanism underlying this unexpected phenomenon?

The immunohistochemically detectable amount of extracellular apoB, indicative for the presence of LDL, was not decreased here. Thus, the invasion of LDL into the subendothelial space – as a prerequisite for atherogenesis – must have occurred but did not induce the same extent and quality of atherosclerosis as observed in the control animals. The reduction of intracellular apoprotein B to immunohistochemically undetectable levels in probucol-treated animals implies that antioxidative protection of LDL might adversley affect the scavenger pathway to a considerable extent. There could be additional effects of probucol on the lipid metabolism within the vessel wall, such as a facilitated lipid transfer [14, 17, 20, 30, 52].

The question remains how those plaques that can still be detected in probucol-treated animals develop despite of the lack of an excessive accumulation of foam cells. It is conceivable that a cholesterol level beyond a threshold is required for this process. This in combination with a minimal oxidation of cholesterol or LDL [2, 8, 33], which may occur even in the presence of probucol within the atherosclerotic plaque [31], might affect a small number of macrophages. Actually, macrophages were still detectable in lesions after probucol treatment in our study. Such minimal changes might suffice to bring on the sequence of events leading to atherosclerotic lesions [38] as a sort of a trigger-mechanism. The intent should be to block this proliferative response of smooth muscle cells, which, as indicated above, is clearly detectable even under circumstances where the macrophage and foam cell content of atherosclerotic lesions is dramatically reduced. An interesting experiment would be the application of a combination of probucol with an antiproliferative substance like Etoposide, which has been shown to change the composition of atherosclerotic plaques in cholesterol-fed rabbits in a different manner [10].

In our experiments using the Watanabe animal model both the plaque constituents and the different types of atherosclerotic plaques resemble those in descriptions of the development of this disease in other animal models [11, 12, 36, 37, 41, 42] and humans [43, 44]. Our results support the validity of the WHHL-rabbit as a relevant model system. From studies in humans we know that it is not the absolute size of a plaque which causes its fatal consequences [15, 16, 27], but rather those aspects of the composition and architecture of a lesion that account for complications such as rupture, bleeding and thrombotic occlusion of a vessel. The thickness of the fibrous cap and its content of macrophages as well as the presence of an atheromatous core have been correlated with the vulnerability of individual atherosclerotic lesions [26, 28]. We demonstrate that treatment of WHHL-rabbits with probucol leads to quantitative as well as qualitative alterations of the atherosclerotic phenotype. As these plaques represent more stable lesions, they might be less susceptible to the fatal complications associated with atherosclerosis.

Acknowledgements We thank Dr. Angelika Gebhardt, Dr. Anja Peters and Dr. David Evans for discussion of the manuscript, Konstanze von Bonin-von Ostau for preparation of the histological specimen, J. Koppelmeier for preparation of Figs. 2A, 3, 5 and 6, Dr. J. Dimigen and Mr. W. Conrad for taking care of the animals.

References

1. Ball RY, Carpenter KLH, Mitchinson MJ (1987) What is the significance of ceroid in human atherosclerosis? Arch Pathol Lab Med 111:1134–1140
2. Berliner JA, Territo MC, Sevanian A, Ramin S, Kim JA, Bamshad B, Esterson M, Fogelman AM (1990) Minimally modified low density lipoprotein stimulates monocyte endothelial interactions. J Clin Invest 85:1260–1266
3. Björkhem I, Henriksson-Freyschuss A, Breuer O, Diczfalusy U, Berglund L, Henriksson P (1991) The antioxidant butylated hydroxytoluene protects against atherosclerosis. Arteriosclerosis Thromb 11:15–22
4. Boyd HC, Gown AM, Wolfbauer G, Chait A (1989) Direct evidence for a protein recognized by a monoclonal antibody against oxidatively modified LDL in atherosclerotic lesions from a Watanabe heritable hyperlipidemic rabbit. Am J Pathol 135:815–825
5. Brown MS, Goldstein JL (1986) A receptor mediated pathway for cholesterol homeostasis. Science 232:34–47
6. Buja LM, Kita T, Goldsteil JL, Watanabe Y, Brown MS (1983) Cellular pathology of progressive atherosclerosis in the WHHL rabbit, an animal model of familial hypercholesterolemia. Arteriosclerosis 3:87–101
7. Carew TE, Schwenke DC, Steinberg D (1987) Antiatherogenic effect of Probucol unrelated to its hypocholesterolemic effect: evidence that antioxidants in vivo can selectively inhibit low density lipoprotein degradation in macrophage-rich fatty streaks and slow the progression of atherosclerosis in the Watanabe heritable hyperlipidemic rabbit. Proc Natl Acad Sci USA 84:7725–7729
8. Cushing SD, Berliner JA, Valente AJ, Territo MC, Navab M, Parhami F, Gerrity R, Schwartz CJ, Fogelman AM (1990) Minimally modified low density lipoprotein induces monocyte chemotactic protein 1 in human endothelial cells and smooth muscle cells. Proc Natl Acad Sci USA 87:5134–5131
9. Daugherty A, Zweifel BS, Schonfeld G (1991) The effects of probucol on the progression of atherosclerosis in mature Watanabe heritable hyperlipidemic rabbits. Br J Pharmacol 103: 1013–1018
10. de la Llera-Moya M, Rothblat GH, Glick JM, England JM (1992) Etoposide treatment supresses atherosclerotic plaque development in cholesterol-fed rabbits. Arteriosclerosis 12: 1363–1370
11. Fagiotto A, Ross R, Harker L (1984) Studies of hypercholesterolemia in the nonhuman primate. I. Changes that lead to fatty streak formation. Arteriosclerosis 4:323–340

12. Fagiotto A, Ross R (1984) Studies of hypercholesterolemia in the nonhuman primate. II. Fatty streak conversion to fibrous plaque. Arteriosclerosis 4:341–356
13. Finckh B, Niendorf A, Rath M, Beisiegel U (1991) Antiatherosclerotic effect of probucol in WHHL-rabbits: are there plasma parameters to evaluate this effect? Eur J Clin Pharmacol [suppl 1] 40: S77–S80
14. Franceschini G, Sirtori M, Vaccarino V, Gianfranceschi G, Rezzonico L, Chiesa G, Sirtori CR (1989) Mechanisms of HDL reduction after Probucol. Changes in HDL subfractions and increased reverse cholesterol ester transfer. Arteriosclerosis 9:462–469
15. Fuster V, Badimon L, Badimon JJ, Chesebro JH (1992) The pathogenesis of coronary artery disease and the acute coronary syndromes. N Engl J Med 326:242–250
16. Fuster V, Badimon L, Badimon JJ, Chesebro JH (1992) The pathogenesis of coronary artery disease and the acute coronary syndromes. N Engl J Med 326:310–318
17. Goldberg RB, Mendez A (1988) Probucol enhances cholesterol efflux from cultured human skin fibroblasts. Am J Cardiol 62:57B–59B
18. Goldstein JL, Kita T, Brown MS (1983) Defective lipoprotein receptors and atherosclerosis. Lessons from an animal counterpart of familial hypercholesterolemia. N Engl J Med 309:288–296
19. Guyton JR, Klemp KF, Black BL, Bocan TMA (1990) Extracellular lipid deposition in atherosclerosis. Eur Heart J [suppl] 11:20–28
20. Gwynne JT (1988) Probucol, high density lipoprotein metabolism and reverse cholesterol transport. Am J Cardiol 62: 48B–51B
21. Haberland ME, Fong D, Cheng L (1988) Malondialdehyde-altered protein occurs in atheroma of Watanabe heritable hyperlipidemic rabbits. Science 241:215–218
22. Havel RJ, Yamada N, Shames DM (1989) Watanabe heritable hyperlipidemic rabbit. Animal model for familial hypercholesterolemia. Arteriosclerosis [suppl]9:I-33–I-38
23. Kita T, Nagano Y, Yokode M, Ishii K, Kume N, Ooshima A, Yoshida H, Kawai C (1987) Probucol prevents the progression of atherosclerosis in Watanabe heritable hyperlipidemic rabbit, an animal model for familial hypercholesterolemia. Proc Natl Acad Sci USA 84:5928–5931
24. Kita T, Ishii K, Yokode M, Kume N, Nagano Y, Arai H, Kawai C (1990) The role of oxidized low density lipoprotein in the pathogenesis of atherosclerosis. Eur Heart J 11 [suppl]: 122–127
25. Ku G, Doherty NS, Schmidt LF, Jackson RL, Dinerstein RJ (1990) Ex vivo lipopolysaccharide-induced interleukin-1 secretion from murine peritoneal macrophages inhibited by probucol, a hypocholesterolemic agent with antioxidative properties. FASEB 4:1645–1653
26. Lendon CL, Davies MJ, Born GVR, Richardson PD (1991) Atherosclerotic plaque caps are lokally weakened when macrophages density is increased. Atherosclerosis 87:87–90
27. Little WC, Constantinescu M, Applegate RJ, Klutcher MA, Burrows MT, Kahl FR, Santamore WP (1988) Can coronary angiography predict the site of a subsequent myocardial infarction in patients with mild-to-moderate coronary artery disease? Circulation 78:1157–1166
28. Loree HM, Kamm RD, Stringfellow RG, Lee RT (1992) Effects of fibrous cap thickness on peak circumferential stress in model atherosclerotic vessels. Circ Res 71:850-858
29. Mao SJT, Yates MT, Parker RA, Chi EM, Jackson RL (1991) Attenuation of atherosclerosis in a modified strain of hypercholesterolemic Watanabe heritable hyperlipidemic rabbits with use of a probucol analogue (MDL 29,311) that does not lower cholesterol. Arteriosclerosis Thromb 11:1266–1275
30. Matsuzawa Y, Yamashita S, Funahashi T, Yamamoto A, Tarui S (1988) Selective reduction of cholesterol in HDL2 fraction by probucol in familial hypercholesterolemia and hyperHDL2 cholesteroemia with abnormal cholesteryl ester transfer. Am J Cardiol 62:66B–72B
31. O'Brien K, Nagano Y, Gown A, Kita T,Chait A (1991) Probucol treatment affects the cellular composition but not anti-oxidized low density lipoprotein immunoreactivity of plaques from Watanabe heritable hyperlipidemic rabbits. Arteriosclerosis Thromb 11:751–759
32. Parthasarathy S, Young SG, Witztum JL, Pittman RC, Steinberg D (1986) Probucol inhibits oxidative modification of low density lipoprotein. J Clin Invest 77:641–644
33. Rajavashisth TB, Andalibi A, Territo MC, Berliner JA, Navab M, Fogelman AM, Lusis AJ (1990) Induction of endothelial cell expression of granulocyte and monocyte colony-stimulating factors by modified low-density lipoproteins. Nature 344:254–257
34. Regnström J, Walldius G, Carlson LA, Nilsson J (1990) Effect of probucol treatment on the susceptibility of low density lipoprotein isolated from hypercholesterolemic patients to become oxidatively modified in vitro. Atherosclerosis 82:43–51
35. Regnström J, Nilsson J, Tornvall P, Landou C, Hamsten A (1992) Susceptibility to low-density lipoprotein oxidation and coronary atherosclerosis in man. Lancet 339:1183–1186
36. Rosenfeld ME, Tsukada T, Gown AM, Ross R (1987) Fatty streak initiation in Watanabe heritable hyperlipemic and comparably hypercholesterolemic fat-fed rabbits. Arteriosclerosis 7:9–23
37. Rosenfeld ME, Tsukada T, Chait A, Bierman EL, Gown AM, Ross R (1987) Fatty steak expansion and maturation in Watanabe heritable hyperlipemic and comparably hypercholesterolemic fat-fed rabbits. Arteriosclerosis 7:24–34
38. Ross R (1993) The pathogenesis of atherosclerosis: a perspective for the 1990s. Nature 362:801–809
39. Salonen JT, Ylä-Herttuala S, Yamamoto R, Butler S, Korpela H, Salonen R, Nyyssönen K, Palinski W, Witztum JL (1992) Autoantibody against oxidized LDL and progression of carotid atherosclerosis. Lancet 339:884–887
40. Schwartz CJ (1988) The Probucol experience: a review of the past and a look at the future. Am J Cardiol 62:1B–5B
41. Schwenke DC, Carew TE (1989) Initiation of atherosclerotic lesions in cholesterol-fed rabbits. I. Focal increases in arterial LDL concentration precede development of fatty streak lesions. Arteriosclerosis 9:895–907
42. Schwenke DC, Carew TE (1989) Initiation of atherosclerotic lesions in cholesterol-fed rabbits. II. Selective retention of LDL vs. selective increases in LDL permeability in susceptible sites of arteries. Arteriosclerosis 9:908–918
43. Stary HC (1989) Evolution and progression of atherosclerotic lesions in coronary arteries of children and young adults. Arteriosclerosis [suppl] 9:I-19–I-32
44. Stary HC (1992) Composition and classification of human atherosclerosis lesions. Virchows Arch [A] 421:277–290
45. Steinberg D, Parthasarathy S, Carew TE (1988) In vivo inhibition of foam cell development by probucol in Watanabe rabbits. Am J Cardiol 62:6B–12B
46. Steinberg D, Parthasarathy S, Carew TE, Khoo JC, Witzthum JL (1989) Beyond cholesterol: modifications of low-density lipoprotein that increase its atherogenicity. N Engl J Med 320:915–924
47. Steinberg D, Witztum JL (1990) Lipoproteins and atherogenesis. Current concepts. JAMA 264:3047–3052
48. Steinbrecher UP, Zhang H, Lougheed M (1990) Role of oxidatively modified LDL in atherosclerosis. Free Radiol Biol Med 9:155–168
49. Thyberg J, Hedin U, Sjölund M, Palmberg L, Bottger BA (1990) Regulation of differentiated properties and proliferation of arterial smooth muscle cells. Arteriosclerosis 10:966–990
50. Tsukada T, Rosenfeld M, Ross R, Gown AM (1986) Immunocytochemical analysis of cellular components in atherosclerotic lesions. Use of monoclonal antibodies with the Watanabe and fat-fed rabbit. Arteriosclerosis 6:601–613
51. Watanabe Y (1980) Serial inbreeding of rabbits with heritable hyperlipidemia (WHHL-rabbit): incidence and development of atherosclerosis and xanthoma. Atherosclerosis 36:261–268
52. Yamamoto A, Hara H, Takaichi S, Wakasugi JI, Tomikawa M (1988) Effect of probucol on macrophages, leading to regression of xanthomas and atheromatous vascular lesions. Am J Cardiol 62:31B–36B